Article

Theoretical Study of Cisplatin Binding to Purine Bases: Why Does Cisplatin Prefer Guanine over Adenine?

Mu-Hyun Baik, Richard A. Friesner, and Stephen J. Lippard

J. Am. Chem. Soc., **2003**, 125 (46), 14082-14092• DOI: 10.1021/ja036960d • Publication Date (Web): 28 October 2003

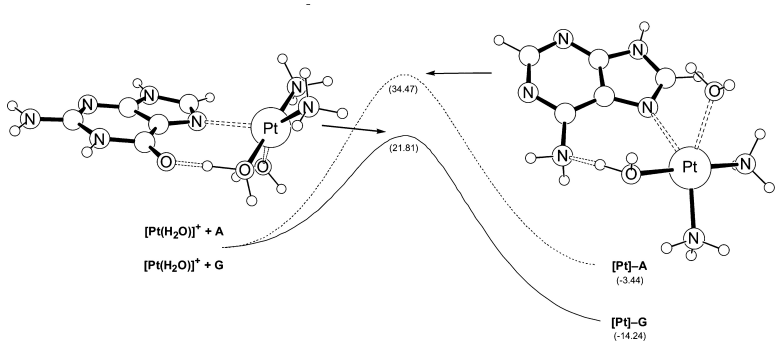

More About This Article

Additional resources and features associated with this article are available within the HTML version:

- Supporting Information
- Links to the 22 articles that cite this article, as of the time of this article download
- Access to high resolution figures
- Links to articles and content related to this article
- Copyright permission to reproduce figures and/or text from this article

View the Full Text HTML

J|A|C|S
ARTICLES
Published on Web 10/28/2003

Theoretical Study of Cisplatin Binding to Purine Bases: Why Does Cisplatin Prefer Guanine over Adenine?

Mu-Hyun Baik,*,†,§ Richard A. Friesner,*,† and Stephen J. Lippard*,‡

Contribution from the Department of Chemistry, Columbia University, New York, New York 10027 and Department of Chemistry, Massachusetts Institute of Technology, Cambridge, Massachusetts 02139

Received June 28, 2003; E-mail: mbaik@indiana.edu; rich@chem.columbia.edu; lippard@lippard.mit.edu

Abstract: The thermodynamics and kinetics for the monofunctional binding of the antitumor drug cisplatin, *cis*-diamminedichloroplatinum(II), to a purine base site of DNA were studied computationally using guanine and adenine as model reactants. A dominating preference for initial attack at the N7-position of guanine is established experimentally, which is a crucial first step for the formation of a 1,2-intrastrand cross-link of adjacent guanine bases that leads to bending and unwinding of DNA. These structural distortions are proposed ultimately to be responsible for the anticancer activity of cisplatin. Utilizing density functional theory in combination with a continuum solvation model, we developed a concept for the initial Pt−N7 bond formation to atomic detail. In good agreement with experiments that suggested $\Delta G^{\ddagger} = \sim$23 kcal/mol for the monofunctional platination of guanine, our model gives $\Delta G^{\ddagger} = 24.6$ kcal/mol for guanine, whereas 30.2 kcal/mol is computed when adenine is used. This result predicts that guanine is 3−4 orders of magnitude more reactive toward cisplatin than adenine. A detailed energy decomposition and molecular orbital analysis was conducted to explain the different barrier heights. Two effects are equally important to give the preference for guanine over adenine: First, the transition state is characterized by a strong hydrogen bond between the ammine-hydrogen of cisplatin and the O═C6 moiety of guanine in addition to a stronger electrostatic interaction between the two reacting fragments. When adenine binds, only a weak hydrogen bond forms between the chloride ligand of cisplatin and the H_2N−C6 group of adenine. Second, a significantly stronger molecular orbital interaction is identified for guanine compared to adenine. A detailed MO analysis is presented to provide an intuitive view into the different electronic features governing the character of the Pt−N7 bond in platinated purine bases.

Introduction

Cisplatin is a widely used anticancer drug[1] that has been particularly successful in treating small cell lung, ovarian, testicular, head, and neck tumors.[2] Since the discovery of this activity some 40 years ago,[3,4] much progress has been made in understanding its mode of action and many details of the mechanism leading to antitumor activity are now well established.[5,6] The primary target of cisplatin is genomic DNA, specifically the N7 position of guanine bases. This point of attack first generates monofunctional adducts, which subsequently closes by coordination to the N7 position of an adjacent purine to afford an intrastrand cross-link.[7,8] This 1,2-intrastrand cross-link bends and unwinds the DNA duplex, suppressing DNA transcription efficiently and ultimately leading to cell death.[9] There is now general agreement that the induced structural distortions are key for the antitumor activity of cisplatin. These intrastrand cross-links are mainly 1,2-d(GpG) and 1,2-d(ApG), with the 1,2-d(GpG) motif being the dominating feature of the platination reaction.[10,11]

Despite significant efforts to design new antitumor agents based on platinum[12,13] and other transition metal complexes[14] in an effort to overcome cisplatin resistance[15,16] or enhance its antitumor activity,[17] there are only a few examples of drugs, namely oxaliplatin,[18,19] carboplatin,[20,21] and nedaplatin,[22] that

† Columbia University.
‡ Massachusetts Institute of Technology.
§ New address: Department of Chemistry & School of Informatics, Indiana University, Bloomington, IN 47405.

(1) *Platinum and Other Metal Coordination Compounds in Cancer Chemotherapy*; Pinedo, H. M., Schornagel, J. H., Eds.; Plenum Press: New York, 1996.
(2) For example, see: Go, R. S.; Adjei, A. A. *J. Clin. Oncol*. **1999**, *17*, 409−422.
(3) Rosenberg, B.; Van Camp, L.; Krigas, T. *Nature* **1965**, *205*, 698.
(4) Rosenberg, B.; Van Camp, L.; Trosko, J. E.; Mansour, V. H. *Nature* **1969**, *222*, 385.
(5) Jamieson, E. R.; Lippard, S. J. *Chem. Rev.* **1999**, *99*, 2467.
(6) Fuertes, M. A.; Alonso, C.; Perez, J. M. *Chem. Rev.* **2003**, *103*, 645.
(7) Bancroft, D. P.; Lepre, C. A.; Lippard, S. J. *J. Am. Chem. Soc.* **1990**, *112*, 6860.
(8) Sherman, S. E.; Lippard, S. J. *Chem. Rev.* **1987**, *87*, 1153.
(9) Mello, J. A.; Lippard, S. J.; Essigmann, J. M. *Biochemistry* **1995**, *34*, 14783.
(10) Fichtinger-Schepman, A. M. J.; van der Veer, J. L.; den Hartog, J. H. J.; Lohman, P. H. M.; Reedijk, J. *Biochemistry* **1985**, *24*, 707.
(11) Eastman, A. *Biochemistry* **1986**, *25*, 3912.
(12) Wong, E.; Giandomenico, C. M. *Chem. Rev.* **1999**, *99*, 2451.
(13) Weiss, R. B.; Christian, M. C. *Drugs* **1993**, *46*, 360.
(14) Clarke, M. J.; Zhu, F. C.; Frasca, D. R. *Chem. Rev.* **1999**, *99*, 2511.
(15) Kelland, L. R. *Drugs* **2000**, *59*, 1.
(16) Giaccone, G. *Drugs* **2000**, *59*, 9.
(17) Judson, I.; Kelland, L. R. *Drugs* **2000**, *59*, 29.
(18) Raymond, E.; Chaney, S. G.; Taamma, A.; Cvitkovic, E. *Ann. Oncol.* **1998**, *9*, 1053.

10.1021/ja036960d CCC: $25.00

are of immediate clinical relevance today. Developing a rational drug design strategy is difficult, in part because a quantitative atomic level understanding of the features controlling the interaction of the Pt moiety with the nucleobases is not available. For example, the preference of guanine over adenine as a target for platination has been suggested to be a consequence of kinetic control,[23] but there is no definitive explanation for the chemical basis of this selective behavior. Similarly unclear are the most salient electronic features that determine the Pt−N bond in microscopic detail. In general, square-planar Pt(II) complexes are relatively inert, and substitution reactions usually occur via Pt-ligand exchange reactions with a trigonal-bipyramidal transition state structure.[24] Consequently, the assertion that the metal binding kinetics[25−28] is more important for biological activity than the overall thermodynamics is intuitively reasonable.[29]

In the past few years, computational methods have made valuable contributions to the collective effort of deriving a better understanding of how cisplatin reacts with DNA. The hydrolysis of cisplatin[30−34] has been intensively studied theoretically at a wide range of different levels of theory. Pt−N bond formation[35,36] and some aspects of the resulting electronic structure changes, such as the influence of platination on base pairing[37−40] or proton affinity,[41,42] have been examined, in addition to many other features.[43−52] Given the chemical similarity of the N7 binding sites in guanine and adenine, it is difficult to envision a fundamentally different Pt-binding mechanism. The observed preference for guanine is thus likely to be the result of a subtle difference.

In the present work, we describe theoretically the initial Pt−N bond formation for guanine and adenine, concentrating on differences in kinetic behavior for the two reactants. It is currently unclear whether the monoaqua[7] complex $[Pt(NH_3)_2Cl(H_2O)]^+$ or the diaqua[25] species $[Pt(NH_3)_2(H_2O)_2]^{2+}$ is most reactive as an electrophile.[53,54] It is likely that both species can and do play a role. We therefore investigated both and identified common mechanistic details as well as distinctive differences that reveal the subtle balance of two main forces governing the interaction of cisplatin with the nucleobases. These are hydrogen bonding and the electronic interaction between the metal center and the lone-pair orbital of N7. Parallel studies aimed at obtaining transition state structures and energies in the gas phase were reported while this manuscript was in preparation.[55] Our transition state structures largely agree with those reported in this study, but our analysis is significantly more detailed. The main goals of the present report are to identify the transition state and to isolate and quantify components of intermolecular forces that govern the energetics.

Computational Details

All calculations were carried out using density functional theory[56,57] as implemented in the Jaguar 4.1 suite[58] of ab initio quantum chemistry programs and the Amsterdam Density Functional 1999.03 package (ADF).[59] Geometries were optimized by using Jaguar and the B3LYP functional[60,61] with the 6-31G** basis set. Platinum was represented by the Los Alamos LACVP** basis,[62−64] which includes relativistic effective core potentials. The energies were reevaluated by additional single point calculations at each optimized geometry using Dunning's[65] correlation consistent triple-ζ basis set cc-pVTZ(-f) with the standard double set of polarization functions. In these single-point calculations, Pt was described by a modified version of LACVP**, designated as LACV3P**, where the exponents were decontracted to match the effective core potential with the triple-ζ quality basis. Vibrational frequency calculation results based on analytical second derivatives at the B3LYP/6-31G** level of theory were used to confirm proper convergence to local minima and maxima for equilibrium and transition state geometries, respectively, and to derive the zero-point-energy (ZPE) and vibrational entropy corrections at room temperature. Solvation energies were evaluated by a self-consistent reaction field (SCRF) approach,[66−68] based on accurate numerical solutions of the Poisson−Boltzmann equation.[69,70] In the results reported below, solvation calculations were carried out at the gas-phase geometry using the

(19) Spingler, B.; Whittington, D. A.; Lippard, S. J. *Inorg. Chem.* **2001**, *40*, 5596.
(20) Wagstaff, A. J.; Ward, A.; Benfield, P.; Heel, R. C. *Drugs* **1989**, *37*, 162.
(21) Teuben, J. M.; Bauer, C.; Wang, A. H. J.; Reedijk, J. *Biochemistry* **1999**, *38*, 12305.
(22) Piccart, M. J.; Lamb, H.; Vermorken, J. B. *Ann. Oncol.* **2001**, *12*, 1195.
(23) Reedijk, J. *Proc. Natl. Acad. Sci. U.S.A.* **2003**, *100*, 3611.
(24) Deeth, R. J.; Elding, L. I. *Inorg. Chem.* **1996**, *35*, 5019.
(25) Legendre, F.; Bas, V.; Kozelka, J.; Chottard, J. C. *Chem.—Eur. J.* **2000**, *6*, 2002.
(26) Kozelka, J.; Legendre, F.; Reeder, F.; Chottard, J. C. *Coord. Chem. Rev.* **1999**, *192*, 61.
(27) Legendre, F.; Kozelka, J.; Chottard, J. C. *Inorg. Chem.* **1998**, *37*, 3964.
(28) Reedijk, J. *Pure Appl. Chem.* **1987**, *59*, 181.
(29) Scovell, W. M.; O'Connor, T. *J. Am. Chem. Soc.* **1977**, *99*, 120.
(30) Carloni, P.; Sprik, M.; Andreoni, W. *J. Phys. Chem. B* **2000**, *104*, 823.
(31) Zhang, Y.; Guo, Z. J.; You, X. Z. *J. Am. Chem. Soc.* **2001**, *123*, 9378.
(32) Tsipis, A. C.; Sigalas, M. P. *THEOCHEM* **2002**, *584*, 235.
(33) Langlet, J.; Berges, J.; Caillet, J.; Kozelka, J. *Theor. Chem. Acc.* **2000**, *104*, 247.
(34) Chval, Z.; Sip, M. *THEOCHEM* **2000**, *532*, 59.
(35) Basch, H.; Krauss, M.; Stevens, W. J.; Cohen, D. *Inorg. Chem.* **1985**, *24*, 3313.
(36) Basch, H.; Krauss, M.; Stevens, W. J.; Cohen, D. *Inorg. Chem.* **1986**, *25*, 684.
(37) Hill, G. A.; Forde, G.; Gorb, L.; Leszczynski, J. *Int. J. Quantum Chem.* **2002**, *90*, 1121.
(38) Cochran, K.; Forde, G.; Hill, G. A.; Gorb, L.; Leszczynski, J. *Struct. Chem.* **2002**, *13*, 133.
(39) Pelmenschikov, A.; Zilberberg, I.; Leszczynski, J.; Famulari, A.; Sironi, M.; Raimondi, M. *Chem. Phys. Lett.* **1999**, *314*, 496.
(40) Burda, J. V.; Sponer, J.; Leszczynski, J. *Phys. Chem. Chem. Phys.* **2001**, *3*, 4404.
(41) Sponer, J. E.; Leszczynski, J.; Glahe, F.; Lippert, B.; Sponer, J. *Inorg. Chem.* **2001**, *40*, 3269.
(42) Burda, J. V.; Sponer, J.; Hrabakova, J.; Zeizinger, M.; Leszczynski, J. *J. Phys. Chem. B* **2003**, *107*, 5349.
(43) Burda, J. V.; Sponer, J.; Leszczynski, J. *J. Biol. Inorg. Chem.* **2000**, *5*, 178.
(44) Deubel, D. V. *J. Am. Chem. Soc.* **2002**, *124*, 5834.
(45) Sponer, J. E.; Glahe, F.; Leszczynski, J.; Lippert, B.; Sponer, J. *J. Phys. Chem. B* **2001**, *105*, 12171.
(46) Sponer, J.; Sponer, J. E.; Gorb, L.; Leszczynski, J.; Lippert, B. *J. Phys. Chem. A* **1999**, *103*, 11406.
(47) Kozelka, J.; Berges, J. *J. Chim. Phys. Phys. Chim. Biol.* **1998**, *95*, 2226.
(48) Monjardet-Bas, V.; Elizondo-Riojas, M.-A.; Chottard, J.-C.; Kozelka, J. *Angew. Chem., Int. Ed.* **2002**, *41*, 2998.
(49) Carloni, P.; Andreoni, W. *J. Phys. Chem.* **1996**, *100*, 17797.
(50) Carloni, P.; Andreoni, W.; Hutter, J.; Curioni, A.; Giannozzi, P.; Parrinello, M. *Chem. Phys. Lett.* **1995**, *234*, 50.
(51) Tornaghi, E.; Andreoni, W.; Carloni, P.; Hutter, J.; Parrinello, M. *Chem. Phys. Lett.* **1995**, *246*, 469.
(52) Burda, J. V.; Sponer, J.; Hrabadkova, J.; Zeizinger, M.; Leszczynski, J. *J. Phys. Chem. B* **2003**, *107*, 5349.
(53) Miller, S. E.; House, D. A. *Inorg. Chim. Acta* **1990**, *173*, 53.
(54) Miller, S. E.; House, D. A. *Inorg. Chim. Acta* **1989**, *166*, 189.
(55) Chval, Z.; Sip, M. *Collect. Czech. Chem. Commun.* **2003**, *68*, 1105.
(56) Parr, R. G.; Yang, W. *Density Functional Theory of Atoms and Molecules*; Oxford University Press: New York, 1989.
(57) Ziegler, T. *Chem. Rev.* **1991**, *91*, 651.
(58) *Jaguar 4.1*; Schrödinger, Inc.: Portland, OR, 2000.
(59) Velde, G. T.; Bickelhaupt, F. M.; Baerends, E. J.; Guerra, C. F.; Van Gisbergen, S. J. A.; Snijders, J. G.; Ziegler, T. *J. Comput. Chem.* **2001**, *22*, 931.
(60) Becke, A. D. *J. Chem. Phys.* **1993**, *98*, 5648.
(61) Lee, C. T.; Yang, W. T.; Parr, R. G. *Phys. Rev. B* **1988**, *37*, 785.
(62) Hay, P. J.; Wadt, W. R. *J. Chem. Phys.* **1985**, *82*, 270.
(63) Wadt, W. R.; Hay, P. J. *J. Chem. Phys.* **1985**, *82*, 284.
(64) Hay, P. J.; Wadt, W. R. *J. Chem. Phys.* **1985**, *82*, 299.
(65) Dunning, T. H. *J. Chem. Phys.* **1989**, *90*, 1007.
(66) Tomasi, J.; Persico, M. *Chem. Rev.* **1994**, *94*, 2027.
(67) Cramer, C. J.; Truhlar, D. G. *Structure and Reactivity in Aqueous Solution, ACS Symposium Series 568*; American Chemical Society: Washington, D.C., 1994.
(68) Cramer, C. J.; Truhlar, D. G. *Chem. Rev.* **1999**, *99*, 2161.

6-31G**/LACVP** basis and employing a dielectric constant of $\epsilon = 80.37$ for water. Whereas the accurate computation of absolute solvation energies remains a challenge and potentially requires careful inspection of the empirical parameters, the differential solvation energy is expected to be less sensitive owing to a significant error cancellation when the same empirical parameters are used. Thus, the differential solvation corrections are most likely more reliable than the absolute energies of solvation. Additional single-point calculations on the Jaguar-optimized structures were conducted using ADF to obtain fragment wave functions and to calculate energy decompositions according to the extended transition state (ETS) theory derived and implemented by Ziegler and Rauk.[71−73] In these calculations, a triple-ζ STO basis set is utilized, with one set of polarization functions as provided in the ADF package (Basis Set IV, frozen core), together with the BLYP functional.[61,74] Relativistic effects on Pt are included using the scalar "zeroth-order regular approximation" (ZORA)[75,76] as implemented in ADF. We make use of the restricted spin formalism throughout the whole study, since all molecules and fragments discussed in this work are closed shell species.

Energy Profiles. The reaction energy profiles for the Pt−N7 bond formation were constructed by placing the fully optimized Pt complex and the nucleobase at a Pt···N7 fixed distance of 4 Å and reoptimizing all coordinates. Next, the Pt···N7 distance was decreased in 0.1 Å steps and fixed until a distance of 2.0 Å was reached, while optimizing the positions of all other atoms. The final distance corresponds approximately to that found when the N7-platinated nucleobases are fully optimized. Using the geometry that gave the highest energy as the initial guess, a quadratic synchronous transit (QST)[77] search for the transition state was conducted. In QST the initial part of the transition state, search is restricted to a circular curve connecting the reactant, transition state guess, and product, then the optimizer follows the Hessian eigenvector most similar to the tangent of the circular curve. Vibrational frequency calculations were utilized to confirm the proper convergence to a local maximum.

ZPE corrections, thermal corrections to the enthalpy, entropy terms, and continuum solvation energies are added to give Gibbs free energies for the reaction in solution, which is most appropriate to compare with what is found in experimental studies. Note that the first three terms are gas phase corrections only. The entropy of solvation is implicitly included in the solvation free energy G(Solv) and cannot be separated when a continuum model is used. For a detailed analysis of the reaction energy profile, partitioning of the reaction free energy into an enthalpic and entropic part would be helpful since the former can be directly associated with the electronic energy of the system and, as will be pointed out below, is a key component that gives rise to the difference between guanine and adenine. Thus, it is convenient to introduce a new energy $\Delta H(\mathrm{Sol}) = \Delta H(\mathrm{SCF}) + \Delta G(\mathrm{Solv})$, that is the electronic reaction energy as computed directly in the DFT calculation using the self-consistent-field procedure, $\Delta H(\mathrm{SCF})$, corrected for the free energy of solvation ΔG(Solv). Although $\Delta H(\mathrm{Sol})$ has no rigorous physical meaning, these two terms capture essentially all of the key features that distinguish the two different reactants, whereas all other corrections give rise to a relatively constant shift of energy. All energy components are listed in the Supporting Information.

Scheme 1

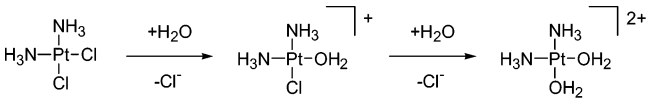

Results and Discussion

Chloroaqua versus Diaqua Complex Binding to Purine Bases. As illustrated in Scheme 1, both chloride ligands act as leaving groups during the aquation of cisplatin, each giving access to a coordination site that can be used to form a Pt−N bond to the nucleobase. As mentioned above, it is currently not established whether the chloroaqua or diaqua complex or both act as the active species for the monofunctional adduct formation. Thus, we carried out two series of calculations using both *cis*-$[Pt(NH_3)_2Cl(H_2O)]^+$ and *cis*-$[Pt(NH_3)_2(H_2O)_2]^{2+}$ as reactants. Although there is no doubt that a Pt−N7 bond forms during initial attack, the exact structure of the monofunctional adduct is not known. In the case of guanine, the oxo group at the C6 position allows for the formation of a hydrogen bond with either the hydrogen of the ammine or that of a water ligand if the Pt complex is in its diaqua form. Similarly, the amino group at the C6 position of adenine has the potential either to act as a hydrogen-bond acceptor or to assume the role of a weak hydrogen-bond donor to the chloride ligand[78,79] in the monoaqua complex. Hydrogen bonds have been implicated to impose both structural[26] and kinetic[23,55,80] control on purine platination. Below, we examine the platination of purine bases in detail and demonstrate quantitatively that hydrogen bonding is one of two main factors that determine both the kinetics and thermodynamics of the platination process.

Pt Binding Energies. To compute the platination energy profiles, it is first necessary to assemble the structures and energies of the reactant. Optimization of the structures of the Pt complexes and the two purine bases is routine, and the optimized structures, given in the Supporting Information, will not be discussed further. The computed energies are listed in Table 1. In the ensuing discussion, it is noteworthy that guanine is substantially better solvated than adenine, which is easy to understand given the high concentration of partial charge at the C6-oxo group. The solvation free energy difference is 8.9 kcal/mol. Solvation energies for the cationic and dicationic Pt complexes follow the expected trend, with −252.4 and −95.6 kcal/mol being computed for the fragments *cis*-$\{Pt(NH_3)_2Cl\}^+$ and *cis*-$\{Pt(NH_3)_2(H_2O)\}^{2+}$, respectively. Values of −220.6 and −78.7 kcal/mol, respectively, are obtained for the analogues with an additional water ligand occupying the empty coordination site.

Figures 1 and 2 show optimized structures for the monofunctional adducts using the monoaqua and diaqua complexes of cisplatin, respectively. Both possible hydrogen-bond patterns involving either the ammine ligand or the Cl/H_2O ligands were considered. The respective electronic energies $\Delta H(\mathrm{SCF})$, solvation and zero-point-energy corrected enthalpies $\Delta H(\mathrm{Sol})$, and the free energy of bond formation in solution, $\Delta G(\mathrm{Sol})$, for each structure are summarized in Table 1. The change in solvation free energy, $\Delta G(\mathrm{Solv})$, is also given. These energies are

(69) Tannor, D. J.; Marten, B.; Murphy, R. B.; Friesner, R. A.; Sitkoff, D.; Nicholls, A.; Ringnalda, M. N.; Goddard, W. A., III.; Honig, B. *J. Am. Chem. Soc.* **1994**, *116*, 11875.
(70) Marten, B.; Kim, K.; Cortis, C.; Friesner, R. A.; Murphy, R. B.; Ringnalda, M. N.; Sitkoff, D.; Honig, B. *J. Phys. Chem.* **1996**, *100*, 11775.
(71) Ziegler, T.; Rauk, A. *Theor. Chim. Acta* **1977**, *46*, 1.
(72) Ziegler, T.; Rauk, A. *Inorg. Chem.* **1979**, *18*, 1755.
(73) Ziegler, T.; Rauk, A. *Inorg. Chem.* **1979**, *18*, 1558.
(74) Becke, A. D. *Phys. Rev. A* **1988**, *38*, 3098.
(75) van Lenthe, E.; Baerends, E. J.; Snijders, J. G. *J. Chem. Phys.* **1993**, *99*, 4597.
(76) van Lenthe, E.; van Leeuwen, R.; Baerends, E. J.; Snijders, J. G. *Int. J. Quantum Chem.* **1996**, *57*, 281.
(77) Peng, C. Y.; Schlegel, H. B. *Isr. J. Chem.* **1993**, *33*, 449.
(78) Brammer, L.; Charnock, J. M.; Goggin, P. L.; Goodfellow, R. J.; Koetzle, T. F.; Orpen, A. G. *J. Chem. Soc., Chem. Commun.* **1987**, 443.
(79) Aullon, G.; Bellamy, D.; Brammer, L.; Bruton, E. A.; Orpen, A. G. *Chem. Commun.* **1998**, 653.
(80) Reedijk, J. *Inorg. Chim. Acta* **1992**, *200*, 873.

Table 1. Energies of Reactants and Fragments

	H(SCF) eV	*G*(Solv) kcal/mol	ZPE kcal/mol	*S* eu	*G*(Gas) eV	*G*(Sol) eV
cis-$\{Pt(NH_3)_2Cl\}^+$	−18840.575	−95.55	50.77	88.949	−18839.523	−18843.667
cis-$\{Pt(NH_3)_2(H_2O)\}^{2+}$	−8385.893	−252.36	66.60	87.607	−8384.138	−8395.081
cis-$[Pt(NH_3)_2Cl(H_2O)]^+$	−20922.981	−78.67	67.54	97.156	−20921.308	−20924.720
cis-$[Pt(NH_3)_2(H_2O)_2]^{2+}$	−10468.770	−220.59	83.17	96.329	−10466.409	−10475.975
guanine	−14768.538	−26.48	73.43	88.678	−14766.500	−14767.649
adenine	−12720.497	−17.56	70.12	84.197	−12718.545	−12719.306

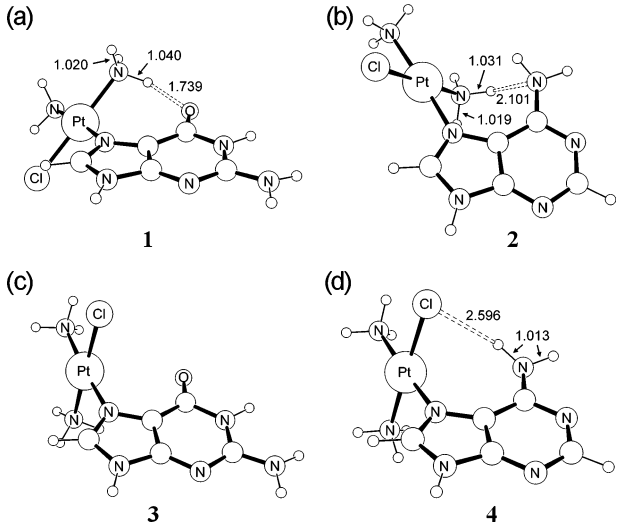

Figure 1. Optimized platination products using chloroaqua complex.

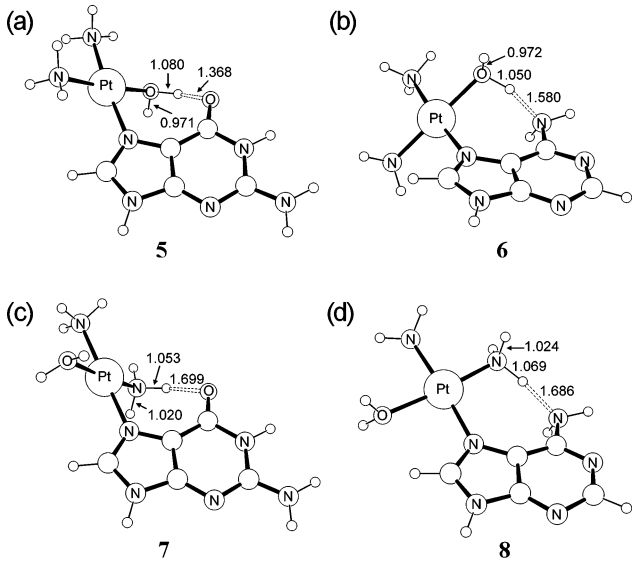

Figure 2. Optimized platination products using diaqua complex.

Scheme 2

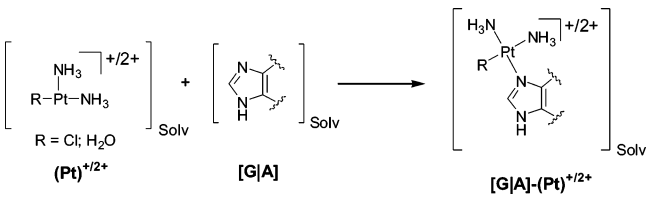

computed using the reaction scheme illustrated in Scheme 2. The additional water ligand for the fully aquated Pt complex acts as the leaving group and is released into bulk solvent space upon completion of the reaction. Thus, it is not treated explicitly but is taken into account through the continuum model to ensure computational consistency.

Table 2. Computed Bond Dissociation Energy Components for the Platination Products Using the Pt-Chloroaqua Complex, as Defined in Scheme 2[a]

	Δ*H*(SCF)	Δ*G*(Solv)	Δ*H*(Sol)	Δ*G*(Sol)
1	−80.69	49.03	−29.82	−16.05
2	−65.47	39.29	−23.45	−8.84
3	−69.80	40.91	−27.74	−14.32
4	−63.37	36.29	−24.92	−11.49

[a] Numbers are defined in Figure 1. All energies are given in kcal/mol.

The uncorrected gas phase energies Δ*H*(SCF) are in fair agreement with computational studies reported previously[43] and predict gas phase electronic energies of −80.7 and −65.5 kcal/mol for the Pt−N7 bonds in platinated guanine and adenine, respectively, using the platinum-monoaqua complex to give species **1** and **2** (Figure 1a and 1b, Table 2). In both structures, the ammine ligands act as hydrogen-bond donors, whereas the oxo and amino groups at the C6 position of the guanine and adenine rings, respectively, are hydrogen-bond acceptors.[81] As expected, the oxo group is a much better hydrogen-bond acceptor than the amino group, and the stronger interaction is reflected in a slightly more pronounced lengthening of the ammine N−H bond in platinated guanine. In structure **1**, the N−H distance is 1.04 Å, whereas 1.03 Å is found in **2** (Figure 1). Although such a differential bond length is irrelevant for practical purposes, the results indicate a subtle trend in the computer model. The spectator ammine N−H bond is computed to be 1.02 Å in both cases. The N−H···O═C6 hydrogen bond is expected to contribute approximately 6−8 kcal/mol to the bond energy of platinated guanine,[82,83] whereas roughly 5 kcal/mol can be estimated for the N−H···NH_2−C7 interaction in platinated adenine. Consequently, the structural isomer **3** (Figure 1c), where the platinum complex has been rotated to avoid a hydrogen bond to the C6-oxo group, is 10.9 kcal/mol higher in energy than **1** (Table 1). Apart from the hydrogen bond, rotation around the Pt−N7 bond results in loss of few kcal/mol intrinsic electronic energy. In the case of platinated adenine, rotation of the cisplatin moiety around Pt−N7 affords species **4** (Figure 1d), in which a favorable electrostatic interaction between the chloride ligand and amino hydrogen at the C6 position gives rise to some compensation for the loss of the stronger hydrogen bond in **2**, resulting in only a 2.1 kcal/mol preference for isomer **2** over isomer **4**. This interaction is a weak hydrogen bond, and we observe practically no N−H bond lengthening effect since both hydrogen atoms of the amino group display the same bond distances of 1.013 Å.

(81) Luisi, B.; Orozco, M.; Sponer, J.; Luque, F. J.; Shakked, Z. *J. Mol. Biol.* **1998**, *279*, 1123.
(82) Vargas, R.; Garza, J.; Friesner, R. A.; Stern, H.; Hay, B. P.; Dixon, D. A. *J. Phys. Chem. A* **2001**, *105*, 4963.
(83) Dixon, D. A.; Dobbs, K. D.; Valentini, J. J. *J. Phys. Chem.* **1994**, *98*, 13435.

Addition of solvation energies results in a significant correction of the binding energies in both absolute numbers and the relative ordering. Overall, platination is accompanied by a significant loss of solvation energy, 35−50 kcal/mol, which is not surprising given the loss of solvent accessible surface upon forming one product molecule from two reactants. In addition, we found a more interesting differential solvation effect. Because of the high charge concentration at the oxo group in guanine, it is notably better solvated, with a solvation energy of −26.5 kcal/mol compared to −17.6 kcal/mol for adenine, as already noted (Table 1). Upon platination and formation of the strong hydrogen bond, the partially negative oxo moiety is no longer accessible to solvent to the same extent. As a consequence, the loss of solvation energy upon adduct formation is 49.0 kcal/mol in the case of guanine, whereas only 39.3 kcal/mol is lost by adenine. This concept of counterbalancing a more pronounced energy gain through formation of a stronger hydrogen bond by a similarly strong loss of solvation energy is a general feature and must be taken into account when estimating the relative stabilities of the adducts.

A convincing example of how these two antagonistic effects determine the overall stability can be seen by comparing the platinated adenine isomers **2** and **4**. Although the stronger hydrogen bond in **2** gives rise to its electronic preference over **4**, the partial shielding of the ammine group from solvation also results in a greater loss of solvation energy. As a result, the formation of adduct **4** is 3.0 kcal/mol less uphill if only solvation energies are taken into account. Adding ZPE corrections inverts the energetic ordering for isomers **2** and **4** in the ΔH(Sol) space, with binding energies of −23.5 and −24.9 kcal/mol for **2** and **4**, respectively. If entropy corrections are added to give the free energy of binding in solution, ΔG(Sol), the preference for **4** increases further resulting in an overall preference of 2.6 kcal/mol for the isomer without the ammine−amino hydrogen bond. The entropic preference is a direct result of the less strong interaction of the chloride ligand with the amino hydrogen compared to the moderately strong hydrogen bond between the ammine hydrogen and the amino nitrogen.

Similarly intuitive is the substantial difference in solvation free energy ΔG(Solv) of 8.1 kcal/mol between the two platinated guanine products **1** and **3**. The complete lack of any hydrogen bonds in **3** gives rise to a much greater exposure of the partially charged functional groups of the adduct to solvents. The resulting larger solvation energy in turn gives a smaller solvation energy penalty of 40.9 kcal/mol in **3** compared to 49.0 kcal/mol in **1**. The magnitude of this differential effect, roughly 10 kcal/mol, makes it clear that hydrogen bonding and solvation energy loss are comparable and that both must be considered. In the case of guanine, where a strong hydrogen bond is formed between the ammine hydrogen and the C6-oxo group, solvation and entropy effects are not sufficient to overturn the energetic preference for **1**. The energy difference is notably smaller, however, with an overall $\Delta\Delta G$(Sol) of 1.7 kcal/mol compared to the difference in purely electronic energy of $\Delta\Delta H$(SCF) = 10.9 kcal/mol.

In summary, we find a preference for the hydrogen-bonded structure **1** over the alternative structure **3** when guanine reacts with the Pt-chloroaqua complex, which is an expected result.[23] The magnitude of the preference for this structural motif is smaller than expected due to solvation and entropy terms, however. For the monofunctional adduct with adenine, we find that the hydrogen-bonded structure **2** is only favored electronically, and differential solvation and entropy terms give rise to a thermodynamic preference for structure **4**. In **4**, a purely electrostatic interaction of the chloride ligand with the amino-hydrogen has replaced the stronger hydrogen bond involving the ammine hydrogen. If the lowest energy structures for the monofunctional adducts **1** and **4** are compared, we find that platination of guanine is thermodynamically preferable by 4.6 kcal/mol, with a binding free energy of −16.1 kcal/mol compared to −11.5 kcal/mol when adenine is the reactant. This energy difference is appreciably smaller than the gas phase values that predict a preference of 17.3 kcal/mol for guanine.

Table 3. Computed Bond Dissociation Energy Components for the Platination Products Using the Pt Diaqua Complex, as Defined in Scheme 2[a]

	ΔH(SCF)	ΔG(Solv)	ΔH(Sol)	ΔG(Sol)
5	−121.85	92.08	−28.42	−14.24
6	−95.68	75.37	−18.02	−3.44
7	−116.25	89.62	−24.96	−11.72
8	−82.33	71.52	−8.62	6.32

[a] Numbers are defined in Figure 2. All energies are given in kcal/mol.

Figure 2 and Table 3 summarize the structures and energies when the Pt diaqua complex is used as reactant. In this case, a water ligand acts as a strong hydrogen-bond donor and dominates the relative energetics of the possible isomers. Structure **5**, in which the Pt-moiety is oriented such as to allow the water ligand to interact with the C6-oxo group (Figure 2a), is preferred electronically (ΔH(SCF)) by 5.6 kcal/mol over structure **7**, where a weaker ammine-H-to-oxo-O interaction is present (Figure 2c). Addition of solvation and entropy effects decreases the preference in free energy to 2.5 kcal/mol. Similar effects are present in the two possible structures of the adenine adduct. Structure **6**, where the water ligand is the hydrogen-bond donor instead of the ammine group as in structure **8**, is the lower energy isomer both in ΔH(SCF) and ΔG(Sol) domains. The antagonistic trends between hydrogen-bond strengths and solvation energy loss described above for the Pt-chloroaqua complex are also present. The isomers with stronger hydrogen bonds, **5** and **6**, are associated with larger losses of solvation energy compared to structures **7** and **8**, respectively (Table 3). Interestingly, the thermodynamic preference for guanine over adenine platination is significantly greater when the Pt diaqua complex is used as the electrophile. The binding free energy in solution ΔG(Sol) is −14.2 kcal/mol for the guanine-Pt adduct **5**, whereas −3.4 kcal/mol is computed for the adenine-Pt adduct. Furthermore, when the second possible structure with the weaker hydrogen bond, structure **8**, is considered, platination of adenine in solution is computed to be an uphill process. Here the electronic binding energy of 82.3 kcal/mol is unable to compensate for the loss of solvation energy of 71.5 kcal/mol, and the loss of entropy that amounts to 14.9 kcal/mol.

Transition States. Whereas the model described above is reasonable for evaluating the thermodynamics for Pt−N bond formation in solution, it is not appropriate for examining the kinetics of the reaction for mainly two reasons. First, conventional electronic structure methods for locating transition states do not allow a routine description of intermolecular bond formation/cleavage reactions because the potential energy

Scheme 3

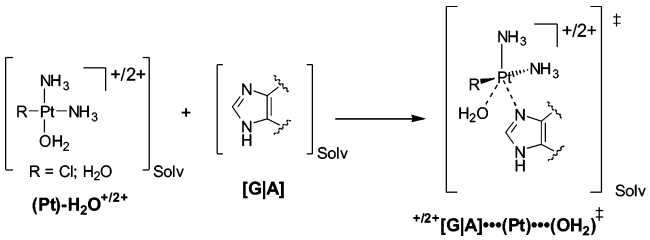

surface does not display a local maximum if only electronic energies are considered.[84,85] The bond formation is a monotonically downhill process on the enthalpic energy space. To obtain a proper transition state, entropy terms that favor the dissociated state have to be included. Second, it is not realistic to model the reacting cisplatin as a $(Pt)^+$ fragment (Scheme 2), because the empty coordination site is occupied by a tightly bound water ligand, which must be treated as a part of the continuum solvent for computational consistency. Square-planar Pt(II) complexes are well-known, however, to undergo associative ligand substitution reactions via a trigonal-bipyramidal transition state. Thus, it is crucial to include the water ligand for a realistic simulation of the kinetics of Pt−N bond formation, as illustrated in Scheme 3. Even if the entropy corrections were introduced for the transition state search, the neglect of an explicitly bound water molecule to the Pt center would not allow a realistic transition state to be identified. The structure of the trigonal-bipyramidal transition state as sketched in Scheme 3 is expected to be dominated by electronic energies, thus making standard quantum mechanical transition state optimization a reasonable protocol if the tightly bound water is included as a ligand.

It is important to recognize that the overall thermodynamics of bond formation cannot be evaluated reliably if the water ligand is treated explicitly, owing to a nontrivial error in this model. The tightly bound water ligand becomes an explicit solvent molecule upon completion of the reaction. In our model, the water molecule will stay loosely bound to the platinated product complex. By placing the product−water complex in a dielectric continuum, we are mixing an explicit solvent with a continuum model, which is problematic by default. In principle, it is necessary to sample a large number of possible product−water complexes and ensemble average over these configurations to obtain a more acceptable estimate for the portion of the energy that the one solvent molecule contributes to the overall solvation. One of the main reasons continuum solvation models deliver acceptably accurate results is that solvation effects are treated in a consistent manner to promote error cancellation. Thus, the model chemistry outlined in Scheme 3 is only reasonable for obtaining the transition state but not well suited for evaluating the overall thermodynamics.

Scheme 4 illustrates the possible structures for the transition states that we have sampled. Analogous to the different structural motifs for the platination product, there are two possible orientations of the Pt-moiety for each adduct structure. The energies of these possible transition states are listed in Table 4. For structure **3TS**, where the chloroaqua complex attacks guanine without the assistance of an ammine-H-to-C6-oxo

Scheme 4

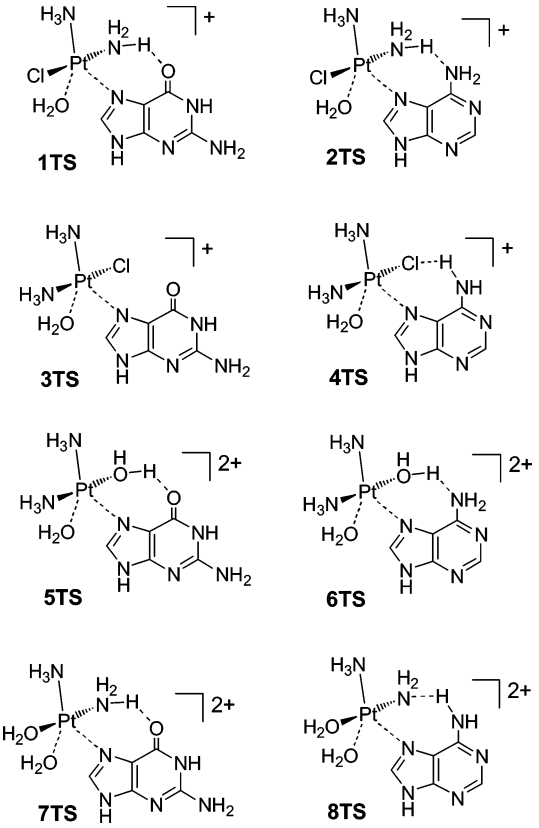

Table 4. Computed Bond Dissociation Energy Components for the Transition States, as Defined in Scheme 3[a]

	Δ*H*(SCF)	Δ*G*(Solv)	Δ*H*(Sol)	Δ*G*(Sol)
1TS	−20.15	32.12	11.86	24.48
2TS	−0.42	22.34	22.64	34.70
3TS				
4TS	−0.71	18.33	18.09	30.62
5TS	−55.37	66.04	8.81	21.81
6TS	−26.15	47.05	20.97	34.47
7TS	−46.05	59.90	13.39	25.63
8TS	−17.13	41.51	24.84	37.56

[a] All energies are given in kcal/mol.

hydrogen bond, we were unable to locate a proper transition state[86] and concluded after much experimentation that the hydrogen-bond assisted transition state **1TS** is the only possible pathway for the addition of the Pt-chloroaqua complex to guanine. As illustrated in Figure 3, the transition state is characterized by the familiar trigonal-bipyramidal structural motif typical for an associative ligand exchange mechanism. At the transition state, the Pt−N7 bond has started to form at a distance of 2.560 Å that is approximately 0.5 Å longer than the final distance in the adduct **1**, while the $Pt-OH_2$ bond is halfway broken at a distance of 2.450 Å. These structural features are in good agreement with those in a recent computational study.[55] As pointed out above, the transition state structure is largely determined by a strong hydrogen bond between the ammine-H and the C6-oxo group of the guanine fragment. The N−H bond distance, which can be taken as an approximate reporter for the extent of hydrogen bonding, is 1.043 Å, and the H···O

(84) Lorant, F.; Behar, F.; Goddard, W. A.; Tang, Y. C. *J. Phys. Chem. A* **2001**, *105*, 7896.
(85) Truhlar, D. G.; Garrett, B. C.; Klippenstein, S. J. *J. Phys. Chem.* **1996**, *100*, 12771.
(86) Attempts to optimize the transition state geometry consistently produced the structure **1TS**.

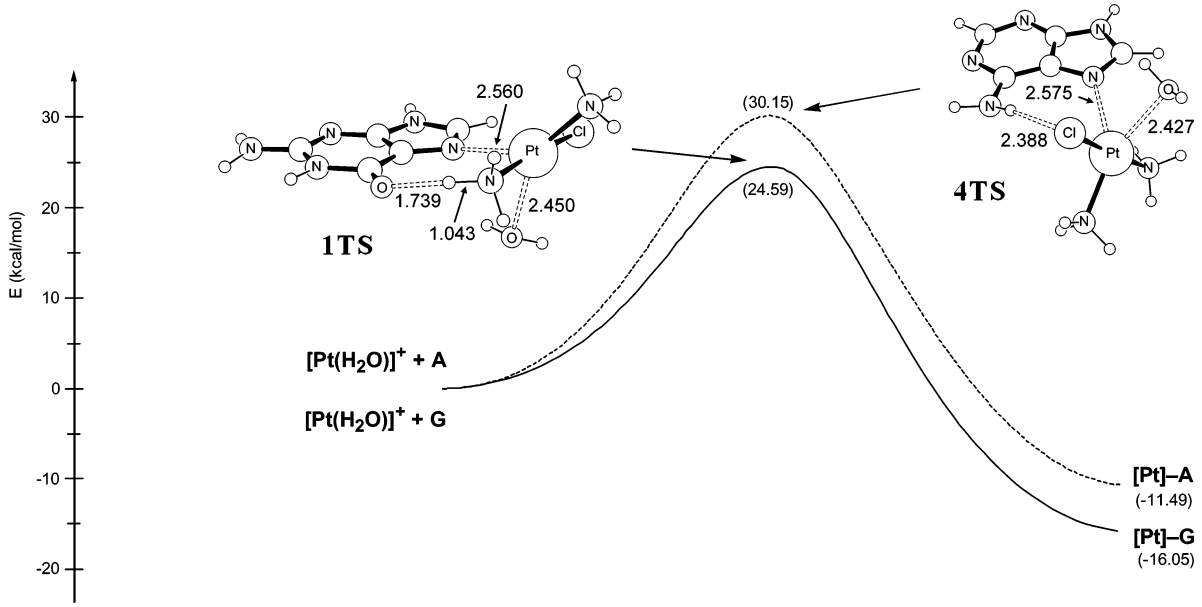

Figure 3. Computed platination reaction profiles. The free energies of activation $\Delta G^{\dagger}$(Sol) are given in parentheses. The energy components of the solvation energy corrected "enthalpy" of activation $\Delta G^{\dagger}$(Sol) are also shown and given in brackets.

distance is 1.739 Å, indicating that the hydrogen bond has been formed to a full extent at the transition state.

In the case of adenine, the two possible structures differing by the Pt ligand that serves as hydrogen-bond donor gave proper transition states geometries, **2TS** and **4TS**,[87] also displaying trigonal-bipyramidal coordination geometry around Pt. Unlike what is described above for the products, the electronic energy ΔH(SCF) indicates that the two isomers are isoenergetic with ΔH(SCF) = −0.4 and −0.7 kcal/mol for **2TS** and **4TS**, respectively (Table 4). As observed for the products, solvation prefers structure **4TS** where only 18.3 kcal/mol is lost, whereas loss of solvation adds 22.3 kcal/mol to the total energy of **2TS**. The final free energies of activation for the platination of adenine are 34.7 and 30.6 kcal/mol for **2TS** and **4TS**, respectively. Thus, our calculation suggests that adenine platination by the Pt-chloroaqua complex is not hydrogen-bond controlled, such that the structure without the possible and stronger hydrogen bond between the ammine-ligand on Pt and the amino-group at the C6 position of the purine ring is preferred both kinetically and thermodynamically when solvation and entropy corrections are taken into account. This result is unexpected, because the ammine-H-to-C6-amino hydrogen bond was frequently implicated in the literature.[23]

The activation free energy of 24.6 kcal/mol for monofunctional platination of guanine by the chloroaqua complex is in excellent agreement with experimental values of 23.4 kcal/mol extracted from variable temperature ^{195}Pt NMR studies for single-stranded DNA.[7] Furthermore, our calculations suggest that there is a dominating preference for guanine platination when the Pt-chloroaqua complex is the active agent. The transition state energy difference of ∼5 kcal/mol between **1TS** and **4TS**, which translates into 3−4 orders of magnitude faster platination of guanine than adenine, and the thermodynamic preference of similar magnitude for guanine confirm that the primary target for monofunctional adduct formation should be guanine. However, the kinetic barrier of 30.2 kcal/mol for adenine platination is not unreasonable for reactions in biologically relevant conditions. Thus, although not favored in a competitive reaction with guanine sites and intrinsically slow, it is clear that platination of adenine sites is also feasible.

The transition states for the diaqua complex are in principle equivalent to those for the chloroaqua complexes. All transition states have trigonal-bipyramidal geometry. Not surprisingly, there is a significant preference for the water ligand on Pt to serve as the hydrogen-bond donor. The lowest energy barriers for both guanine and adenine platination involve such a hydrogen bond, as illustrated in Figure 4. The reaction barrier for guanine platination is significantly lower for isomer **5TS** with ΔG(Sol) = 21.8 kcal/mol, which is 3.8 kcal/mol lower than for **7TS**, in which the ammine group is the hydrogen-bond donor instead of the water ligand (Scheme 2). Experimentally, the activation barrier at room temperature was determined to be 18.3 kcal/mol,[88] which is in good agreement with our computed value of 21.8 kcal/mol, if the usual uncertainty of approximately ±2 kcal/mol is taken into account. This activation energy is significantly lower than the barrier computed for the reaction by the Pt-chloroaqua complex described above. Platination of adenine is highly disfavored, with the lowest transition barrier being 34.5 kcal/mol for structure **6TS** where the water-ligand acts as the hydrogen-bond donor. Complex **8TS**, in which the ammine-H forms the hydrogen bond, is even less favorable, with ΔG(Sol) = 37.6 kcal/mol. For all practical purposes, these barriers would result in extremely slow reactions, thus predicting that the platination of adenine should not be observable at standard conditions if the diaqua complex is the only active reagent.

Analysis of the Energy Differences. In comparing the different energy terms discussed in detail above, it is apparent that the entropy effects, while significant in magnitude for obtaining realistic absolute values, are not important for understanding the selectivity of the platination reaction for guanine. In all cases entropy corrections shift the overall energy

(87) Structure **4TS** is equivalent to the transition state structure **TSAde1b** reported previously.[55]

(88) Arpalahti, J.; Lippert, B. *Inorg. Chem.* **1990**, *29*, 104.

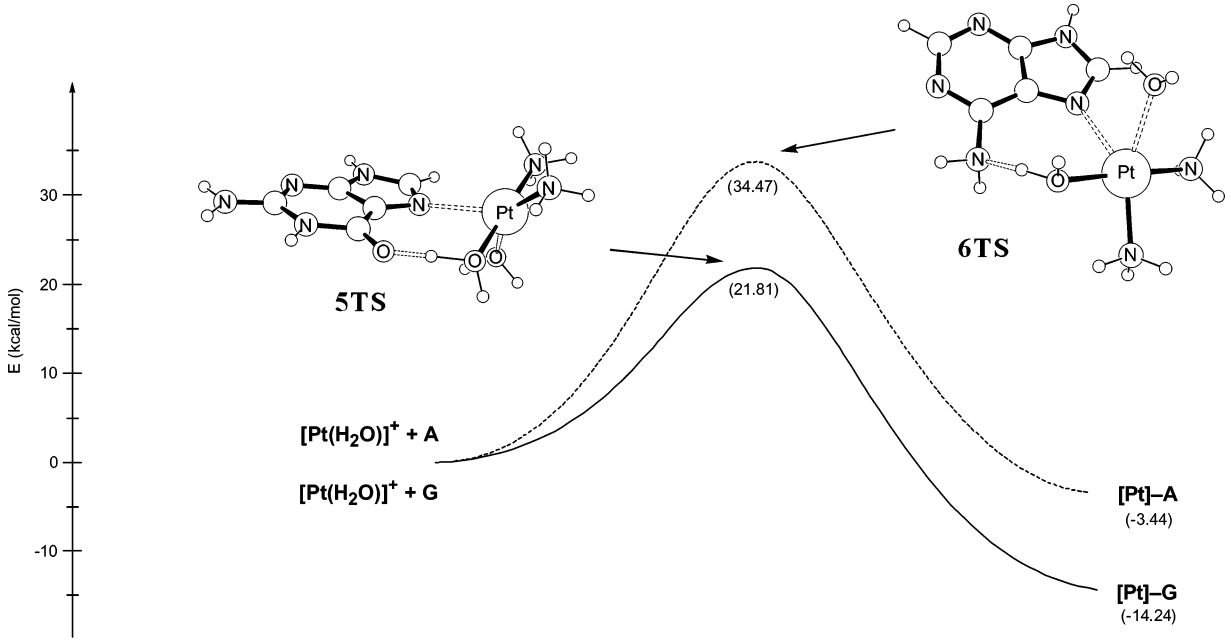

Figure 4. Reaction profile for using the Pt diaqua complex.

uphill by approximately 12−15 kcal/mol, which simply reflects the fact that platination decreases the translational entropy by forming one molecule out of two reactants. The differential ZPE corrections and other terms between the two purine reactants are small and, therefore, do not contribute to a deeper understanding of reactant selectivity.

More specific are the solvation energy trends that are sensitive to the actual structure of the molecule. In our model, we explicitly consider the response of a continuum solvent to structural change of the solute cavity and the extent of electron density exposure at the solute-continuum surface. Specific interactions between highly charged moieties, such as negatively charged phosphate groups, or the fact that the nucleobases are not fully exposed to solvation in DNA have not been included in our model and are potential flaws in our approach. We nonetheless expect a significant degree of error cancellation by employing consistent charge screening, which is key in designing a useful computational model. In general, adduct formation is associated with a solvation energy penalty, which is consistently higher for guanine than for adenine. This trend is an important counterbalance for an intrinsically higher gas phase bond energy of the Pt-guanine compared to the Pt-adenine product and contributes to equalizing the different gas phase reactivities of the purine bases. It is important to recognize that, without the solvent effects, the preference for guanine would be substantially greater and computational models would predict nonrealistic energy differences.

With these trends quantitated in detail, the final step to understanding the reactant specificity lies in examining the great energetic preference of guanine in the ΔH(SCF) domain. The predicted differences are as large as 19.4 and 29.2 kcal/mol between the lowest energy transition states when the active Pt-species are assumed to be chloroaqua and diaqua complexes, respectively.

Energy Decomposition. In addition to lending confidence to our Jaguar-DFT results by reproducing the relative energies with ADF, the fragment calculations routinely available in ADF provide a unique way of decomposing the binding energies in a chemically meaningful manner.[89] This protocol has been discussed in detail in our previous report[90] and elsewhere.[59] Table 5 lists the energy terms according to the Ziegler−Rauk decomposition scheme of the four transition states examined above. The Pt−N7 bond is used to define the two molecular fragments. Note that the definition of bond energy is now slightly different from that used above. Whereas the energies used above are referenced to the fully relaxed dissociation products, the Ziegler−Rauk scheme uses fragments with geometries as found in the original molecule. Thus, the fragments are not at their equilibrium geometry, giving rise to exaggerated bond energies when compared to that of a truly adiabatic bond dissociation energy.[91]

Table 5. Ziegler−Rauk Energy Decomposition of the Pt-[G/A] Interaction in the Transition State Structures[a]

	1TS	4TS	diff	5TS	6TS	diff
ΔE_{Pauli}	58.04	44.41	13.63	93.02	67.63	25.39
$\Delta E_{\text{el-st}}$	−64.76	−41.49	−23.27	−93.78	−61.72	−32.06
$\Delta E_{\text{nonorb-int}}$	−6.72	2.92	−9.64	0.76	5.91	−5.15
$\Delta E_{\text{orb-int}}$	−35.82	−26.05	−9.77	−90.62	−68.24	−22.38
ΔE_{total}	−42.54	−23.14	−19.40	−91.38	−62.33	−29.05

[a] All energies are given in kcal/mol.

The decomposition of the electronic energy reveals that the differential energy of 19.40 kcal/mol separating the two transition states **1TS** and **4TS** reflects equal contributions from $\Delta E_{\text{orb-int}}$, the orbital interaction term, and $\Delta E_{\text{nonorb-int}}$, which is computed as the sum of the Pauli repulsion (ΔE_{Pauli}) and electrostatic energies ($\Delta E_{\text{el-st}}$). $\Delta E_{\text{orb-int}}$ is what is classically

(89) Frenking, G.; Fröhlich, N. *Chem. Rev.* **2000**, *100*, 717.
(90) Baik, M. H.; Friesner, R. A.; Lippard, S. J. *J. Am. Chem. Soc.* **2002**, *124*, 4495.
(91) This energy difference has frequently been termed "preparation energy" and is the energy needed to distort the equilibrium geometries of the dissociated fragments to that found in the adduct structure. For example, whereas H(SCF) for **1TS** was computed to be −20.1 (Table 4), the fragment binding energy ΔE_{total} for the same species is −42.5 kcal/mol (Table 5). All of the relative energy trends observed for the four transition states above are reproduced in this protocol, however. The energy difference between **1TS** and **4TS**, for example, is predicted to be 19.4 kcal/mol using ADF which compares well with the energy difference of 19.7 kcal/mol mentioned above (Table 4).

envisioned as electronic energy, that is, the stabilization energy obtained by favorable interactions between occupied and unoccupied fragment molecular orbitals resulting in a new electronic configuration. The second term, $\Delta E_{\text{nonorb-int}}$, is the result of a balance between the tendency of electron clouds on the molecular fragments to avoid each other (Pauli repulsion) and the electrostatic attraction between partially charged portions of the fragments. In our case, the difference in orbital interaction energies with respect to the two purine reactants is mainly associated with the partial formation of the Pt−N7 bond at the transition state, and the electrostatic energy difference is primarily governed by the favorable interactions between the ammine-H and the oxo group and those between the chloride ligand and the amino-H for the guanine and adenine reactants, respectively. The electrostatic interactions between the metal center and its closest atoms of the purine ring are of a similar order of magnitude in both transition states and cancel each other to a great extent. Thus, $\Delta E_{\text{nonorb-int}}$ is a good indicator for the different hydrogen-bonding strengths and suggests that the kinetic preference for guanine platination is ~50% due to the presence of a hydrogen-bond donor at the ligand directly bound to platinum.

The presence of an $-NHR_2$ group directly attached to the Pt center is one of the empirical anticancer design features that has been widely accepted. Our study confirms this strategy and reveals the reason for it, but it is important to recognize that the orbital interaction term is just as important for the kinetically controlled selectivity. For future rational drug design strategies, the realization of the interplay between these two energy factors gives access to a potentially powerful control mechanism. It is clear that the presence of only one hydrogen-bond donor is required to maintain the favorable electrostatic interaction. The other ammine group is a spectator for the most important electrostatic interaction and consequently should be a prime target for ligand variation in order to change the orbital interaction term without perturbing the hydrogen-bond based electrostatics. This consideration places the "tunable" ammine group at a position trans to the Pt−N7 bond being formed, which is fortuitous in the sense that electronic trans effects in square-planar Pt(II) complexes are well-understood phenomena. On the other hand, it is important to recognize that electrostatic interactions are subject to a powerful and consistent counter-balancing force. Differential solvation energy appears to work against any energetic advantage arising from forming strong hydrogen bonds that usually require highly polarized functional groups. As pointed out above, these groups tend to be highly solvated, and formation of strong hydrogen bonds will be accompanied by loss of solvation. A more systematic examination of a series of different ligands is needed for a better understanding on how to control this balance and exploit it to identify new drug candidates. Such studies are currently in progress in our laboratories.

Explaining the origin of the electronic preference for guanine at the transition state in intuitive terms is not straightforward. We have described the electronics of the platination process in great detail.[90] The molecular orbital interactions are unusually complicated. Intuitively, a donor−acceptor interaction between the occupied N7 lone-pair orbital of the purine reactant and the empty Pt-based $d_{x^2-y^2}$ orbital is expected. Our previous study revealed that, although this picture is largely true, there are a

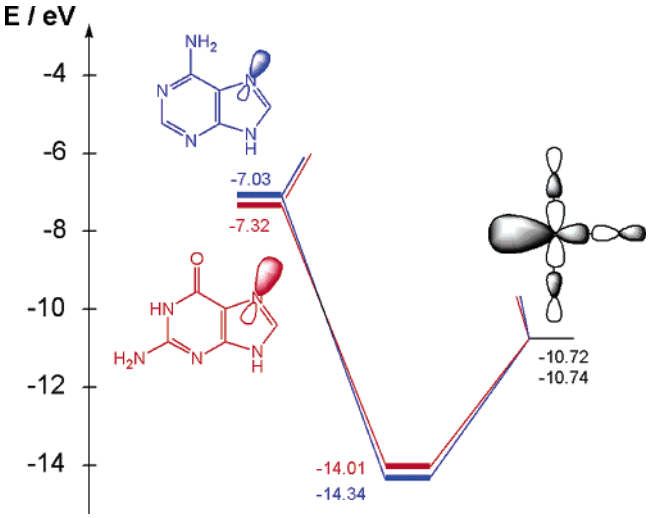

Figure 5. The most important molecular orbital promoting the Pt−N7 bond formation.

number of significant orbital relaxation and reorganization effects at work, which cannot be neglected when dissecting the binding energy in a quantitative fashion. These processes involve metal-based orbitals that are orthogonal to the molecular plane of the Pt fragment and have recently been misinterpreted as π-back-donation components of the Pt−N bond, implicating electron density flow from the metal center to the π^*-orbital of the purine ring.[44,92]

Figure 5 illustrates the intuitive donor−acceptor interaction using a simplified partial MO diagram. The accepting orbital of this interaction is the Pt $d_{x^2-y^2}$ dominated MO, which is the LUMO of the Pt fragment.[90,93] The presence of the electron withdrawing oxo group at the C6 position of the purine ring lowers the energy of the lone-pair orbital at N7 of the purine base. In guanine, this MO has an energy of −6.877 eV, whereas −6.675 eV is obtained for adenine. The iconic representation of the MO is highly simplified for clarity. In reality, the N7 lone-pair orbital mixes with many ring-based orbitals, most notably lone pairs on the nitrogen atoms of the heterocyle, to give a fairly delocalized MO in both guanine and adenine (Figure 6). The isosurface plots reveal a nontrivial and important difference between these two donor orbitals. In guanine, the N7 lone-pair character is clearly the dominating feature of this MO, as indicated by the size of the lone-pair lobe at the N7 position. In adenine, the N7 lone-pair character is also clearly present, but is actually a minor component. This difference is indicated qualitatively in the iconic MO representation in Figure 5. As a consequence, a stronger donor-acceptor interaction between guanine and the Pt fragment is expected owing to better orbital overlap. Indeed, the fragment orbital overlap between the donor−acceptor orbitals is 0.252 and 0.136 in the transition states **1TS** and **4TS**, respectively. These considerations add a nontrivial component to determining the donor ability of the N7 lone pair. Its effect is not simple to trace because changes of the overall MO character, by adding or subtracting atomic orbitals at remote sites, can control the electronic behavior of

(92) For a more detailed discussion, see: Baik, M.-H.; Friesner, R. A.; Lippard, S. J. *Inorg. Chem.*, in press.
(93) Because the distortion towards the trigonal-bipyramidal structure in the transition state is more pronounced in the case of guanine, the orbital energy of this orbital is slightly higher by 0.024 eV, as indicated in Figure 5, but this detail is probably not of practical significance.

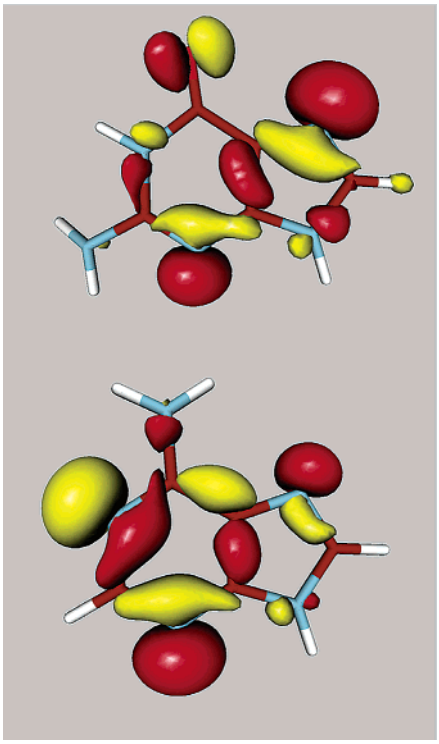

Figure 6. Isosurface plots (Isosurface Value = 0.025 au) of the "lone-pair" orbital that functions as the donor orbital in guanine (top) and adenine (bottom).

this donor orbital significantly. These effects are difficult to predict in a qualitative sense. A more traditional way of rationalizing the donor abilities of lone-pair orbitals is examining their orbital energy. Higher orbital energies that are usually also accompanied by a spatial expansion of the orbital are commonly correlated to stronger electron donating abilities. This rationale would predict that the N7 lone pair in adenine should be a stronger electron donor, which is in part true as indicated by lower orbital energy of the nearly formed σ-bond in the transition state. As shown in Figure 5, the in-phase combination of the donor−acceptor orbital has energies of −14.338 and −14.008 eV for adenine and guanine, respectively. Attempts to rationalize the overall trend found for the orbital interaction energies, $E_{\mathrm{orb-int}}$, discussed above with the pairwise acceptor−donor interaction alone do not lead to a satisfactory concept, as is demonstrated by the fact that this pairwise interaction would predict a larger $E_{\mathrm{orb-int}}$ for adenine.

A last feature to consider is that the transition state structures are not exactly equivalent. Most importantly, the N7−Pt distances are slightly different in the two transition states, as shown in Figure 3. If guanine is the reactant, the N7−Pt distance is 2.560 Å, whereas 2.575 Å is obtained for adenine. This result reflects both the stronger hydrogen bond discussed above, which promotes a more compact transition state geometry for guanine, and the shape of the donor orbital shown in Figure 6, affording a larger thermodynamic driving force for maximizing the donor−acceptor overlap. Thus, the transition state for the platination of guanine is "late" when compared to that of adenine, considering the main reaction coordinate to be the N7−Pt vector.

Similar trends are observed for the Pt diaqua complex. Because of the higher charge of the Pt fragment, all energies are increased in magnitude significantly (Table 5). The electrostatic component of the differential energy is decreased substantially and a preference for guanine is only 5.2 kcal/mol compared to the 9.6 kcal/mol preference when the chloroaqua complex was the electrophile. This difference is easy to understand and reflects the strong versus moderately strong hydrogen bonds in **5TS** and **6TS**, respectively. In this case, the orbital interaction component is dominating, with a differential energy contribution of 22.4 kcal/mol. This trend is in principle understandable in view of the fact that the dicationic Pt fragment should be a better electrophile such that the orbital interaction term, containing the donor−acceptor interaction, is expected to play a much more significant role. For a complete and intuitive understanding of the subtle mechanisms that ultimately give rise to a stronger orbital interaction energy for guanine, it is necessary to study a larger number of purine-based reactants and to quantify how variations of functional groups influence the makeup of the important MOs, in particular the primary donor orbital shown in Figure 6. Such a study is in progress in our laboratories.

Conclusions

We have examined the binding of the two possible hydrolysis products of cisplatin, $[Pt(NH_3)_2Cl(H_2O)]^+$ and $[Pt(NH_3)_2(H_2O)_2]^{2+}$, to the nucleobases guanine and adenine. Our results demonstrate good agreement with experimental observations that guanine is the preferred reactant for platination. The N7 platination of guanine is both thermodynamically and kinetically more favorable. After considering a number of possible transition states, all of which display a trigonal-bipyramidal coordination geometry at platinum, we found that a strong hydrogen bond between the hydrogen of the ammine ligand on Pt and the oxo group at the C6 position of guanine plays a pivotal role in stabilizing the Pt-guanine adduct by comparison to the Pt-adenine adduct, accounting for approximately 50% of the differential energy when the Pt-chloroaqua complex is the reactant. The second half of the energetic preference originates from a stronger electronic interaction between the Pt-moiety and guanine. Interestingly, the Pt-adenine adduct in which the Pt-ammine ligand serves as the hydrogen-bond donor is energetically not favorable compared to an isomer where the amino functionality on the C6 position acts as a hydrogen donor to the chloride ligand, instead. This counterintuitive ordering of the relative stability is the result of a greater solvation and entropy component.

If the diaqua complex is used as the platination agent, both the kinetic and thermodynamic preferences for guanine are increased significantly, by 9.6 and 7.4 kcal/mol, respectively. Thus, we predict a higher selectivity for guanine if the diaqua complex is the active platinum complex. Analyzing the differential energy components, we have identified possible leads for rational design strategies by recognizing that only one of the ammine ligands is involved in hydrogen bonding at the transition state, whereas the other is positioned trans to the Pt−N7 bond that is being formed. Thus, functionalization of one ammine ligand might allow for tuning the electronic properties of the Pt−N7 bond formation process without perturbing the hydrogen-bond donation abilities of the second ammine to the C6-oxo group. This idea will be examined in detail in future work in a framework of a broader electronic structure investigation that aims at deriving a quantitative characterization of the

differential orbital interaction energies between the transition states found for the two different purine bases.

Acknowledgment. This work was supported by grants from the NIH to R.A.F. (GM 40526) and to S.J.L. (CA 34992). Computational resources were provided by the NPACI program under a grant to R.A.F. and by the NCRR division of NIH (P41 RR06892).

Supporting Information Available: Coordinates for optimized geometries of all calculations reported herein, calculated vibrational frequencies of all systems, and itemized energies (PDF). This material is available free of charge via the Internet at http://pubs.acs.org.

JA036960D